Ref. Ares(2022)2398534 - 31/03/2022

Ponderful

PONDS FOR CLIMATE

Deliverable D3.6

Protocol for Downscaling Global Climate Data

Pond Ecosystems for Resilient Future Landscapes in a Changing Climate

European Commission

This project has received funding from the European Union's Horizon 2020 Research and Innovation Programme under Grant Agreement No ID 869296

University of Vic – Central University of Catalonia (Spain) – Prof. Sandra Brucet (PI, Project coordinator), Dr. Diana van Gent (Project Manager)

IGB im Forschungsverbund Berlin (Germany) – Dr. Thomas Mehner (PI, Task lead 2.4)

Katholieke Universiteit Leuven (Belgium) – Dr. Luc De Meester (PI, WP2 coordinator)

Haute Ecole Spécialisée de Súisse occidentale (Switzerland) – Dr. Beat Oertli (PI, WP4 coordinator)

Universitat de Girona (Spain) –Dr. Dani Boix (PI)

Ecologic Institut gemeinnützige GmbH (Germany) – Dr. Manuel Lago (PI, Task lead 1.4)

University College London (UK) –Dr. Carl Sayer (PI)

Middle East Technical University (Turkey)– Dr. Meryem Beklioğlu (PI)

CIIMAR - Interdisciplinary Centre of Marine and Environmental Research (Portugal) –Dr. José Teixeira (PI, WP5 co-coordinator)

Aarhus University (Denmark) – Dr. Thomas A. Davidson (PI)

Uppsala University (Sweeden) –Dr. Malgorzata Blicharska (PI)

Bangor University (UK) – Dr. Sopan Patil (PI)

Technical University of Munich (Germany) – Dr. Johannes Sauer (PI, Task lead 1.6)

I.S.A.R.A. – **Institut Supérieur d'Agriculture Rhône-Alpes (France)** – Dr. Joël Robin (PI)

Middle East Technical University (Turkey) – Dr. Meryem Beklioğlu (PI)

Freshwater Habitats Trust (UK) – Dr. Jeremy Biggs (PI, WP5 co-coordinator)

Universidad de la República (Uruguay) – Dr. Matías Arim (PI)

Randbee Consultants SL (Spain) – Juan Arevalo Torres (PI)

Amphi International APS (Denmark) – Lars Briggs (PI, Task lead 5.4)

Ponderful

Authors:
Zuhal Akyurek, Çağrı Karaman, Mustafa Berkay Akpınar

Contributors:
Matias Arim, Sopan Patil

Document title: Deliverable D3.6 – Protocol for Downscaling Global Climate Data
Document Type: Deliverable

WP No: 3
WP Title: Scenarios and Modelling
WP Lead: BU

Date: 31 March 2022
Document Status: Final version

This project has received funding from the European Union's Horizon 2020 Research and Innovation Programme under Grant Agreement No ID869296

European Commission

Table of Contents

List of Tables

List of Figures

1. Executive Summary

This protocol presents the methodology to downscale the Global Climate Models' results to be used at pondscape scale. After giving the information about global climate models, how to download and map the global climate model results, the bias corrections are presented. Lastly, the downscaling methodology proposed is explained in this report.

2. Introduction

Global Climate Models (GCM) are mathematical representations of the major climate system components of Earth and relevant systems. GCM comprehends and makes predictions by getting the information of climate components and their interactions including atmosphere, land surface, ocean and water bodies.

GCMs can be divided as energy balance models, intermediate complexity models and general circulation models. Energy balance models are mostly utilized for forecasting climate change of Earth via the energy budget of Earth. Likewise, intermediate complexity models are very similar to energy balance ones. On the other hand, they also consider some geographical features for large scale scenarios like atmospheric composition changes over time. Lastly, general circulation models can be counted as the most complex and accurate models. These kinds of models use three dimensional grids and observe so many components like carbon cycle, water circulations, chemistry of atmosphere. However, this results in a requirement of a large amount of computing power and time. Schematic view of the processes and interactions are depicted in Figure 1.

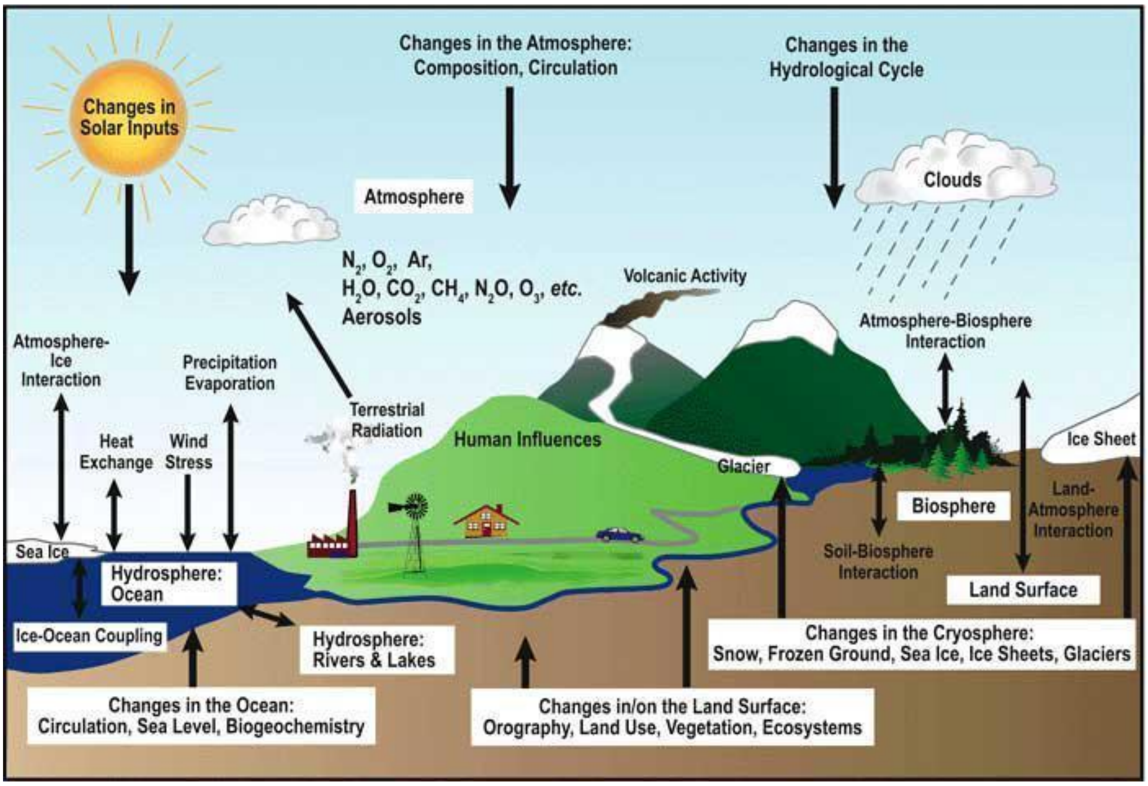

Figure 1. Depiction of the processes and interactions for the global climate models (Le Treut et al., 2005).

Coupled Model Intercomparison Project (CMIP) [1] is run by the World Climate Research Program (WCRP) Working Group on Coupled Modelling (WGCM) with the central goal of advancing scientific understanding of the Earth system. Since 1995, CMIP has coordinated climate model experiments involving multiple international modeling teams worldwide and has developed in phases (Taylor et al., 2012). CMIP model simulations have also been regularly assessed as part of the Intergovernmental Panel on Climate Change (IPCC) Climate Assessments Reports and various national assessments.

Recently the sixth phase of (CMIP6) is available with numerous academic and operational institutions around the world whose outputs of climate models are shared with a common set of inputs. Participating model groups are given in Table 1.

[1] https://www.wcrp-climate.org/wgcm-cmip

Table 1. CMIP6 Participating Model Groups (Eyring et al., 2016).

	Institution	**Country**		**Institution**	**Country**		**Institution**	**Country**
1	AWI	Germany	12	DOE	USA	23	MRI	Japan
2	BCC	China	13	EC-Earth-Cons	Europe	24	NASA-GISS	USA
3	BNU	China	14	FGOALS	China	25	NCAR	USA
4	CAMS	China	15	FIO-RONM	China	26	NCC	Norway
5	CasESM	China	16	INM	Russia	27	NERC	UK
6	CCCma	Canada	17	INPE	Brazil	28	NIMS-KMA	Republic of Korea
7	CCCR-IITM	India	18	IPSL	France	29	NOAA-GFDL	USA
8	CMCC	Italy	19	MESSY-Cons	Germany	30	NUIST	China
9	CNRM	France	20	MIROC	Japan	31	TaiESM	Taiwan, China
10	CSIR-CSIRO	South Africa	21	MOHC	UK	32	THU	China
11	CSIRO-BOM	Australia	22	MPI-M	Germany	33	Seoul Nat.Uni	Republic of Korea

Latest studies for the performance of CMIP6 for different outputs revealed that CMIP6 can capture the trends of global surface temperatures due to the observational data (Fan et al., 2020) and the extreme precipitations (Dong and Dong, 2021). It has been concluded that CMIP6 highly outperforms CMIP5. Additionally, CMIP6 reduces the intermodal variability and error in precipitation and temperature (Bağçaci et al., 2021). However, researchers should remember that these models may have some uncertainties especially for regional studies (You et al., 2021).

Inherently, these models have coarser resolutions and may be impractical for local observations/predictions. Therefore, researchers and scientists have developed and utilized 'downscaling' methods to use the coarse data for local sites.

Downscaling is the procedure of compiling the information from large scales to the local scales. Main aim is shifting the coarse resolution of climate models to the finer and locally utilizable spatial data. This process is divided as dynamical and statistical downscaling which are commonly used in different disciplines like climatology, remote sensing and meteorology (Peng et al., 2017).

Dynamical downscaling drives higher resolution of extrapolated simulations of climate models. These models are sometimes called as 'regional climate models (RCM)'. They utilize the information of global models as boundary conditions and reproduce local climates. However, they are computationally intensive.

Statistical downscaling is a method to develop a relationship between the past observed climate data (from local stations most of the time) and the relevant output of climate models. Researchers have downscaled emission scenarios, land surface temperatures and rainfalls for many models and many decades owing to its less computational efforts (Fowler et al., 2007). On the other hand, there are some important highlights and recommendations to consider for a fine scale, downscaled model. Firstly, there are assumptions and approximations which means there are uncertainties inherently. Secondly, the representation might be beyond the capacity of GCM outputs. Lastly, downscaling can be both spatially and temporally. The combination of their outputs might increase the accuracy of prediction for climate change. The components for developing statistically or dynamically downscaled climate projections are summarized in Figure 2.

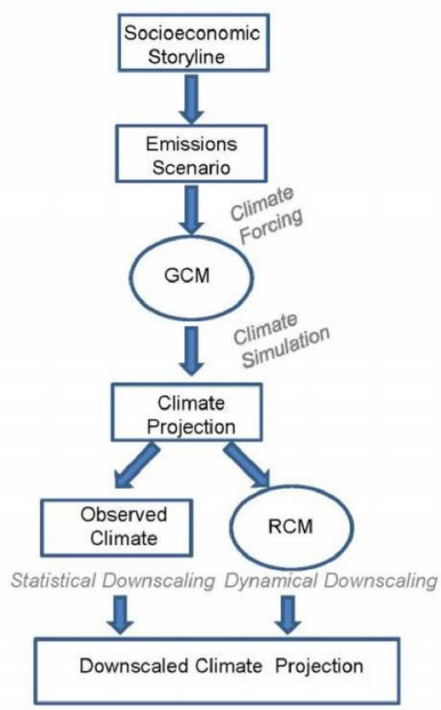

Figure 2. Components for developing climate projections (Daniels et al., 2012).

Statistical downscaling has numerous techniques to carry out the process. They are mostly simple to implement but require a considerable amount of high-quality observational data. These methods can be classified in three groups as ‘linear methods’, ‘weather classifications’, ‘weather generations’.

Linear methods help to downscale the models using the linear relation between the predictors and predictands. They are quite straightforward and commonly used. However, they require normally distributed predictor and predictands values which may be a problematic constraint in some data types. For example, rainfall might be very though to downscale with linear methods, because the distribution of rainfall is mostly not normal and most researchers concluded that the rainfall value distributions of gamma and log-normal give the best fits (Sharma & Singh, 2010). Some examples for linear methods are delta method, linear and multiple linear regression, canonical correlation analysis (CCA) and singular value decomposition (SVD).

Weather classifications are utilized for the process of predictions for local variables on large-scale atmospheric states. The future states from GCMs match with the similar historical atmospheric results. All distribution types are convenient for these methods. However, a large amount of data is needed (e.g., 30 years of daily data for the region of interest). Lastly, these methods are computationally demanding. Some examples for weather classification methods are analog methods, clusters, artificial neural networks (ANN) and other machine learning methods like self-organizing map (SOM).

Weather generators are typically used in temporal downscaling like sequences of daily weather variables (precipitation, humidity etc.) which correspond to monthly or annual averages. They are quite useful for some impact models that need temporal downscaling, which GCMs cannot reliably provide. Some examples for weather generators are MarkSim GCM, nonhomogeneous hidden Markov model (NHMM) and other stochastic weather generators like LARS-WG.

A summary table for statistical downscaling categories and their predictors/predictands with advantages and disadvantages can be seen in Table 2.

Table 2. Statistical downscaling categories and their predictors/predictands with advantages and disadvantages (Trzaska & Schnarr, 2014).

Category	Predictor & Predictand	Advantages	Disadvantages
Linear Methods - *Spatial*	Same type of variable (e.g., both Monthly temperature, both monthly precipitation)	• Relatively straight-forward to apply • Employs full range of available predictor variables	• Requires normality of data (e.g., monthly temperature, monthly precipitation, long-term average temperature) • Cannot be applied to non-normal distributions (e.g., daily rainfall) • Not suitable for extreme events.
Weather Classification - *Spatial and temporal*	Variables can be of the same type or different (e.g., both monthly temperature or one monthly wind and the other monthly precipitation)	• Relatively straight- forward to apply • Employs full range of available predictor variables • Yields physically interpret- able linkages to surface climate • Versatile, i.e., can be applied to both normally and non-normally	• Requires normality of data (e.g., monthly temperature, monthly precipitation, long-term average temperature) • Cannot be applied to non-normal distributions (e.g., daily rainfall) • Not suitable for extreme events • Requires additional step of weather type classification
Weather Generator- *Spatial and temporal*	Same type of variable, different temporal scales (e.g., predictor is monthly precipitation and predictand is daily precipitation)	• Able to simulate length of wet and dry spells • Produces large number of series, which is valuable for uncertainty analysis • Production of novel scenarios	• Data-intensive • Only some weathers generators can check for the coherency between multiple variables (e.g., high insolation should not be predicted on a rainy day) • Requires generation of multiple time-series and statistical post-processing of results

Lastly, benefits, drawbacks and application fields of dynamical and statistical downscaling are summarized in Table 3.

Table 3. Benefits, drawbacks and application fields of dynamical and statistical downscaling (Patz et al., 2005).

Downscaling Type	Benefits	Drawbacks	Applications
Dynamical Downscaling	• Simulates Climate Mechanisms • No a priori assumptions about how current and future climate are related • 'State of the science' tools • Continually advancing computers are making RCMs faster and cheaper to run • Encourages collaborations between health and climate scientists	• Expensive, in terms of computer resources and professional expertise • Results may be sensitive to uncertain parameterizations • Biases in the GCM (providing boundary conditions) may propagate to regional scale • Output from models may not be in a format well-suited to health analysis – additional data processing often required	• Health responses associated with climate extremes and nonlinear variability • Data-poor areas • Connecting outcomes with climate processes • Include land-use impacts on climate or health outcomes
Statistical Downscaling (especially regression methods)	• Much cheaper (runs quickly on desktop computers with free software) • Builds on the statistical expertise common among public health researchers • May correct for biases in GCM • Allows for the assessment of climate results over a range f GCMs and emission scenarios	• Assumes relationships between local and large-scale climate remain constant • Does not capture climate mechanisms • Not well suited to capturing variance or extreme events	• Climate means, and variability with some limitations • Data-rich regions, especially Northern Hemisphere mid-latitudes • Compare present with projected climate in a consistent framework • Test a range of inputs • Variable scales, down to individual measurements sites

3. Method

3.1. Literature on statistical downscaling methods

There are some recent studies about the regression/machine learning based techniques for statistical downscaling processes. For example, the comparison between the techniques of artificial neural network (ANN), Bayesian (BAYE), classification and regression trees (CART), K nearest neighbor (KNN), random forest (RF), and support vector machine (SVM) were observed (Liu et al., 2020) for the downscaling of surface soil moisture data. It has been concluded that Random Forest achieved the excellent performance by using the land surface temperature (LST), normalized difference vegetation index (NDVI), albedo, digital elevation model (DEM), and geographic coordinates as explanatory variables.

Another study for the spatial downscaling (Karbalaye Ghorbanpour et al., 2021) compared the performances of the support vector machine (SVM), random forest (RF), geographically weighted regression (GWR), multiple linear regression (MLR) and exponential regression (ER) for the downscaling of ‘Tropical Rainfall Measuring Mission’ precipitation data. It has been concluded that SVM and RF-based models resulted in considerably higher accuracy. Similarly, GWR outperformed MLR and ER because GWR algorithm can capture the spatial variation between the precipitation and the environmental factors.

Statistical downscaling for the temperature and their relevant performances were compared (Pang et al., 2017). Surface temperature values were obtained for local sites by using the random forest (RF), multiple linear regression (MLR) and artificial neural networks (ANN). It has been concluded that random forest gives the best results for the downscaling of temperature with high accuracy.

Different GCM results (precipitation, temperature etc.) may need different techniques for statistical downscaling. On the other hand, random forest (RF), geographically weighted regression (GWR) and support vector machine (SVM) give higher accuracies for most of the time.

Additionally, some other interpolation techniques with supportive co-variables to increase accuracy of resampling can be implemented for climate analysis. One of the valuable methods might be co-kriging. Co-Kriging (CK) is an extension of ordinary kriging in which additional observed variables (known as co-variate which are often correlated with the variable of interest) are used to improve the precision of the interpolation of the variable of interest.

Recent studies on kriging-based interpolation/downscaling show that kriging is quite useful from a statistical approach for getting higher resolution data. One of the recent studies about a spatial-temporal Co-kriging method (Yang et al., 2021), which is referred to as ST-Co-kriging method. This method extends traditional Co-kriging from a spatial domain to a space-time domain and takes into account the spatial and temporal covariance and cross covariance structures in the spatial-temporal data assimilation. They have used daily MODIS images at 250 m and 500 m spatial resolution being assimilated for a reduced revisit cycle to generate daily reflectance and Normalized Difference Vegetation Index (NDVI) at 30 m spatial resolution. Their process chart can be seen in Figure 3.

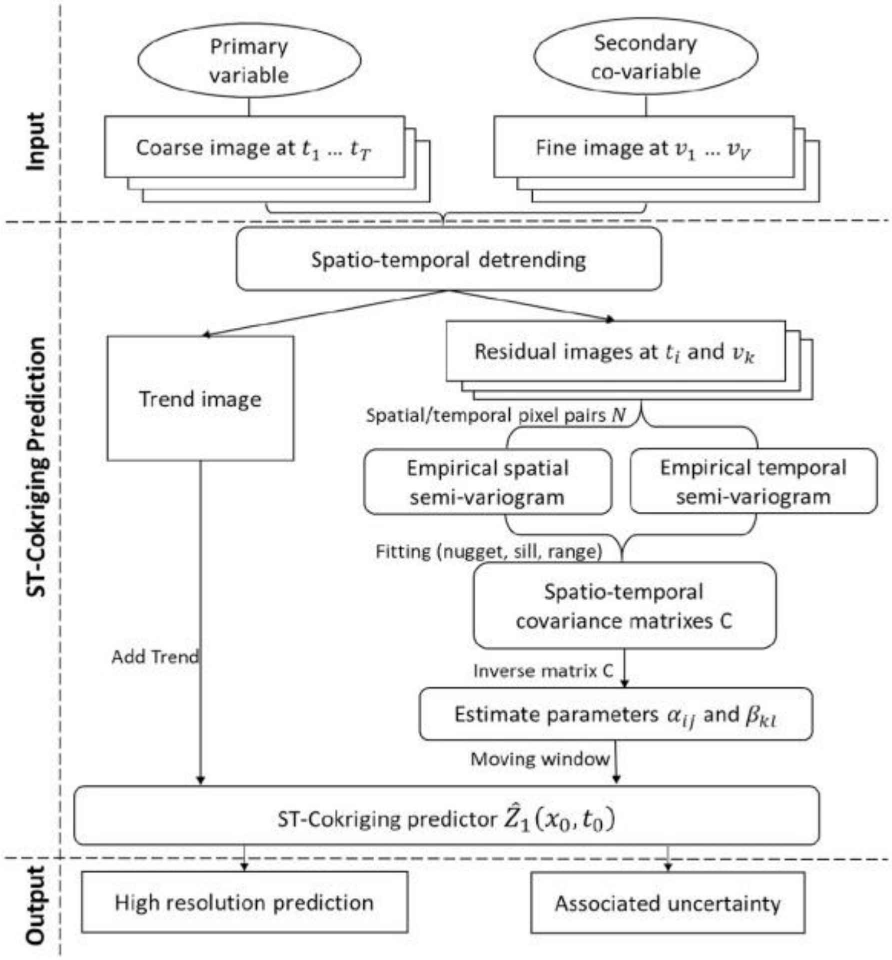

Figure 3. Process flow of Co-kriging implementation for high resolution image (Yang et al., 2021).

One of the other studies for the projection of the long-term ungauged rainfall (Tukimat et al., 2019) indicates that kriging based interpolation can produce reliable long-term rainfall generation for unmeasured observation locations. The GIS-Kriging method used to treat the ungauged station. The interpolation results produced by GIS-Kriging at ungauged station was slightly similar to the control station with %MAE was 16.1% (historical comparison) and 15.3% (projection comparison). It has proven that the integrated model can provide the rainfall trend at ungauged stations reaches 84% of accuracy. Bostan et al. (2012) compared multiple linear regression (MLR), ordinary kriging (OK), regression kriging (RK), universal kriging (UK), and geographically weighted regression (GWR) in mapping the spatial distribution of annual precipitation for Turkey and found that universal kriging is the most accurate method. Kara et al. (2016) used the geographically weighted regression (GWR) method, based on local implications from physical geographical variables, to downscale climate change impacts to a small-scale catchment.

3.2. Choosing the appropriate GCM to downscale

Eight CMIP6 GCMs, which were previously used for Turkey (Bağçaci et al., 2021), are chosen as global climate models (MRI-ESM2, MPI-ESM1-2-HR, CNRM-ESM2-1, NOR-ESM2-MM, HADGEM-GC-31-MM, ACESS CM-2, GFDL-ESM4 and CNRM-CM6-1-HR) to present the methodology. Details about these models are given in Table 4. All the CMIP6 outputs are downloaded using Earth System

Grid Federation (ESGF) LiU datanode[2]. The models provide data for three periods - the historical period (1979-2014), the validation period (2015-2020), and the future prediction period (2021-2100). IPCC describes five different Socio-economic Pathways (SSP) for future society. SSP1 for sustainable development, SSP2 for middle-of-the-road development, SSP3 for regional rivalry, SSP4 for inequality and SSP5 for fossil-fueled development (Kriegler et al., 2017; Riahi et al., 2017). For the future predictions, we ran IPCC SSP2-4.5 and SSP5-8.5 simulations.

Table 4. Global Circulation Models

Global Circulation Model	**Nominal Resolution (km)**	**Ensemble**	**Historical Simulation**	**Future Simulation**		**Parameter**
				SSP 245	**SSP 858**	
CNRM-ESM2-1	250	r1i1p1f2	+	+	+	Near-Surface Air Temperature
MPI-ESM1-2-HR	100	r1i1p1f1	+	+	+	Near-Surface Air Temperature
MRI-ESM2	100	r1i1p1f1	+	+	+	Near-Surface Air Temperature
NOR-ESM2-MM	100	r1i1p1f1	+	+	+	Near-Surface Air Temperature
ACCESS CM-2	250	r1i1p1f1	+	+	+	Precipitation
GFDL-ESM4	100	r1i1p1f1	+	+	+	Precipitation
CNRM-CM6-1-HR	50	r1i1p1f2	+	NA	+	Precipitation
HADGEM-GC-31-MM	100	r1i1p1f3	+	NA	+	Precipitation

3.3. Comparison for the historical period

i- Ground Stations

The GCM results must be compared with the ground observations for the historical period to determine the model performance. Since the climate models have different spatial resolutions, a proper grid system is created. To select the best representative stations over the region, digital elevation model (NASA Shuttle Radar Topography Mission 1 Second Digital Elevation Model) can be used. The idea is to select the representative ground station having the same altitude with the median altitude of the GCM grid.

Eight different grid systems are generated since all eight climate models have different vertical and horizontal resolutions. The median elevation is found for every grid over Turkey, then the closest station in terms of elevation is used to represent each grid as can be seen in Figure 4 for only CNRM-ESM2-1 as an example. A total of 588 different stations are selected for eight different GCMs.

[2] https://esg-dn1.nsc.liu.se/projects/esgf-liu/

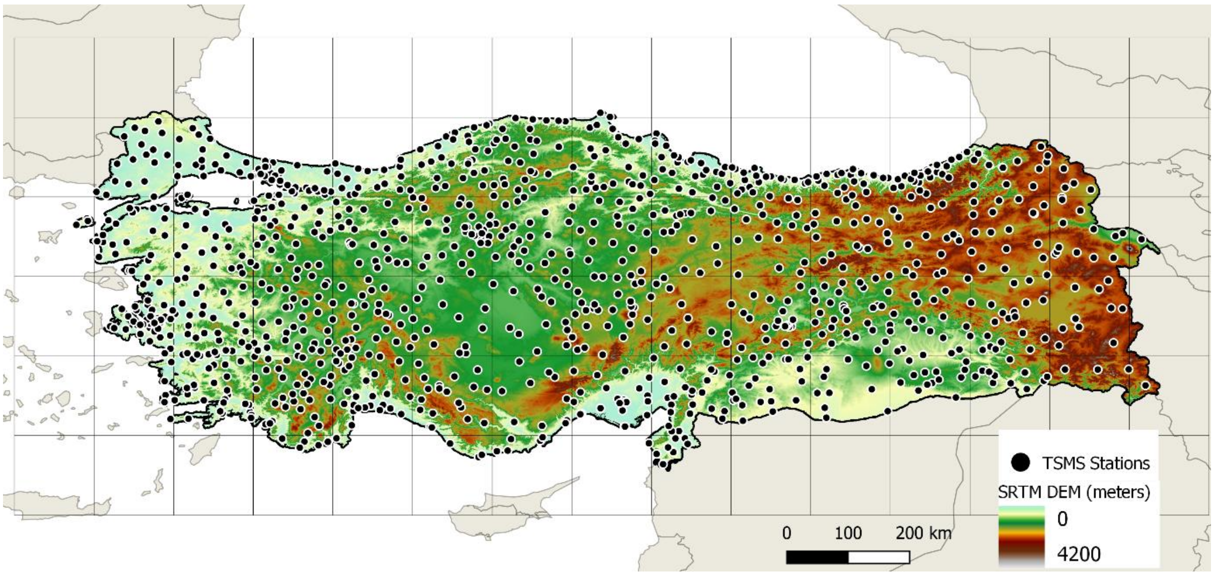

Figure 4. Grid level of CNRM-ESM2-1 GCM and meteorological stations over Turkey.

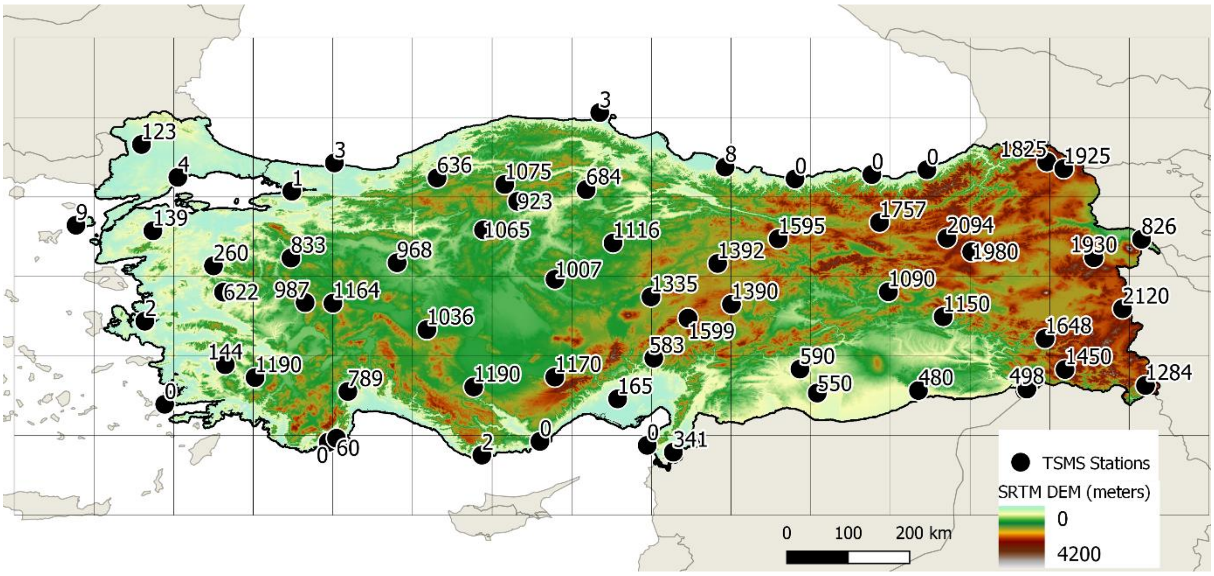

Figure 5. Representative Ground Stations for CNRM-ESM2-1 (Values represent station elevation).

ii- ERA5 reanalysis products

If the continuous data from the ground stations do not exist, ERA5 Reanalysis [3](*The ERA5 global reanalysis*, 2020) data can be used. ERA5 Reanalysis hourly data is aggregated to daily data for comparison with the daily values of GCMs. Recent studies (Bağçaci et al., 2021) have validated ERA5 data as ground-based meteorological observation data for both temperature and precipitation over Turkey. Thus, the ERA5 dataset is used in the further steps.

Since the spatial resolution of ERA5 (temperature and precipitation) is higher than CMIP6 models, zonal statistics such as minimum, maximum, mean and median are calculated for each corresponding grid of CMIP6. Several performance parameters have been examined in order to compare daily ERA5 and

[3] https://cds.climate.copernicus.eu/cdsapp#!/dataset/reanalysis-era5-single-levels

CMIP6 historical data. The suitable model can be selected by considering the following performance metrics.

- Modified Index of agreement (md)
- Normalized Root Mean Square Error (nRMSE)
- Pearson correlation coefficient (R) and
- Kling-Gupta Efficiency (KGE).

Modified Index of Agreement:

md is first introduced by Legatas (Legates & McCabe, 1999) as:

$$md = 1.0 - \frac{\sum |O_i - P_i|}{\sum |P_i - \underline{O}| + |O_i - \underline{O}|} \tag{1}$$

The benefit of md is explained as that errors and differences are given appropriate weighting and are not inflated by their square values (Bağçaci et al., 2021). It varies from 0 (no agreement) and 1 (perfect agreement).

Normalized Root Mean Square Error (nRMSE):

nRMSE is used for absolute error measure for our case in order to be consistent with the previous studies (Bağçaci et al., 2021).

$$nRMSE = \frac{\left[\frac{1}{N}\sum (P_i - O_i)^2\right]^{\frac{1}{2}}}{O\_ - O\_min} \tag{2}$$

Pearson correlation coefficient (R):

$$R = \frac{cov(P,O)}{\sigma_o * \sigma_P} \tag{3}$$

Kling Gupta Efficiency (KGE):

KGE is first introduced by Gupta in 2009 (Gupta et al., 2009). KGE is calculated using three components (Koch et al., 2018) namely, Person Correlation Coefficient, Bias ratio and variability ratio.

$$KGE = 1 - \sqrt{(\alpha - 1)^2 + (\beta - 1)^2 + (\gamma - 1)^2} \tag{4}$$

$$\beta = \frac{\mu_G}{\mu_O} \tag{5}$$

$$\gamma = \frac{\frac{\sigma_G}{\mu_G}}{\frac{\sigma_O}{\mu_O}} \tag{6}$$

where α is Pearson correlation Coefficient between historical CMIP6 values and ERA5 Reanalysis product, β is bias ratio and γ is variability ratio. The KGE values vary from minus infinity to 1, where 1 indicates higher model performance.

3.4. Bias Correction

The analysis is performed using daily values from the historical period (1979-2014). The bias of the GCM results must be checked. If there is bias in the model results, they must be corrected.

The bias in temperature data can be corrected by using a simple seasonal bias correction method (Soriano et al., 2019).

$$T_{Bias\ Corrected\ (Model),daily} = T_{Model,daily} - \Delta T_{monthly} \tag{7}$$

where ΔT is the difference between the mean temperature of the climate model and the observations in the corresponding month. The difference between climate model results and observations (monthly data) was subtracted from the daily raw values of the model to get bias-adjusted daily temperature values for the historical period.

Biases in the precipitation data can be corrected by using the linear scaling method (Ines & Hansen, 2006).

$$P_{Bias-Corrected\ (Model),daily} = P_{Model,daily} * \left(\frac{\underline{P}_{Observation}}{\underline{P}_{Model}}\right) \tag{8}$$

where, $P_{Bias-Corrected\ (Model),daily}$ is the bias-corrected daily precipitation of the model prediction, $P_{Model,daily}$ is the daily precipitation model value, and $\underline{P}_{Observation}$ is the means of the observation and model values for the corresponding month. The ratio between climate model results and observations was multiplied by the model's daily raw values to get bias-adjusted precipitation values for the historical period.

3.5. Results of ERA5 – CMIP6 comparison

One representative GCM is selected for both temperature and precipitation to present the methodology. All GCMs are compared to ERA5 daily data for historical period (1979-2014). The performance metrics can be presented for each grid for daily temperature and daily precipitation as they are given in Figure 6 and Figure 7, respectively.

CMIP6 original, ERA5 and CMIP6 bias corrected mean annual temperature values can be seen in Figure 8. Values from GCM and Reanalysis outputs are chosen from the best performed grids in terms of modified index of agreement. Those grids can be seen in Figure 6 and Figure 7. After the bias is corrected on daily temperature values, the comparison with the ERA5 data can be performed on monthly basis (Figure 9). It can be seen that CMIP6 temperature values underestimate the temperature throughout all months except September. On daily basis, the bias correction improves the results compared to original CMIP6 temperature values (Figure 10).

Table 5. Comparison of CMIP6 and ERA5 daily data for the period of 1979 – 2014.

CNRM-ESM2 (Temperature)	**Modified Index of Agreement**	**Normalized Root Mean Square Error**	**Pearson R**	**Kling-Gupta Efficiency**
Minimum	0.722	0.086	0.874	0.856
Maximum	0.704	0.092	0.854	0.745
Mean	0.778	0.069	0.892	0.863
Median	0.777	0.070	0.890	0.875
CNRM-ESM2 (Temperature) Bias Corrected	**Modified Index of Agreement**	**Normalized Root Mean Square Error**	**Pearson R**	**Kling-Gupta Efficiency**
Minimum	0.717	0.090	0.869	0.825
Maximum	0.730	0.083	0.876	0.806
Mean	0.796	0.064	0.904	0.900
Median	0.798	0.063	0.906	0.906

ACCESS-CM2 (Precipitation)	**Modified Index of Agreement**	**Normalized Root Mean Square Error**	**Pearson R**	**Kling-Gupta Efficiency**
Minimum	0.219	0.120	0.042	-9.024
Maximum	0.497	0.051	0.069	-0.332
Mean	0.430	0.070	0.065	-0.043
Median	0.415	0.068	0.062	-0.160
ACCESS-CM2 (Precipitation) Bias Corrected	**Modified Index of Agreement**	**Normalized Root Mean Square Error**	**Pearson R**	**Kling-Gupta Efficiency**
Minimum	0.251	0.102	0.055	-6.105
Maximum	0.508	0.050	0.079	-0.399
Mean	0.457	0.063	0.079	0.066
Median	0.445	0.061	0.077	0.056

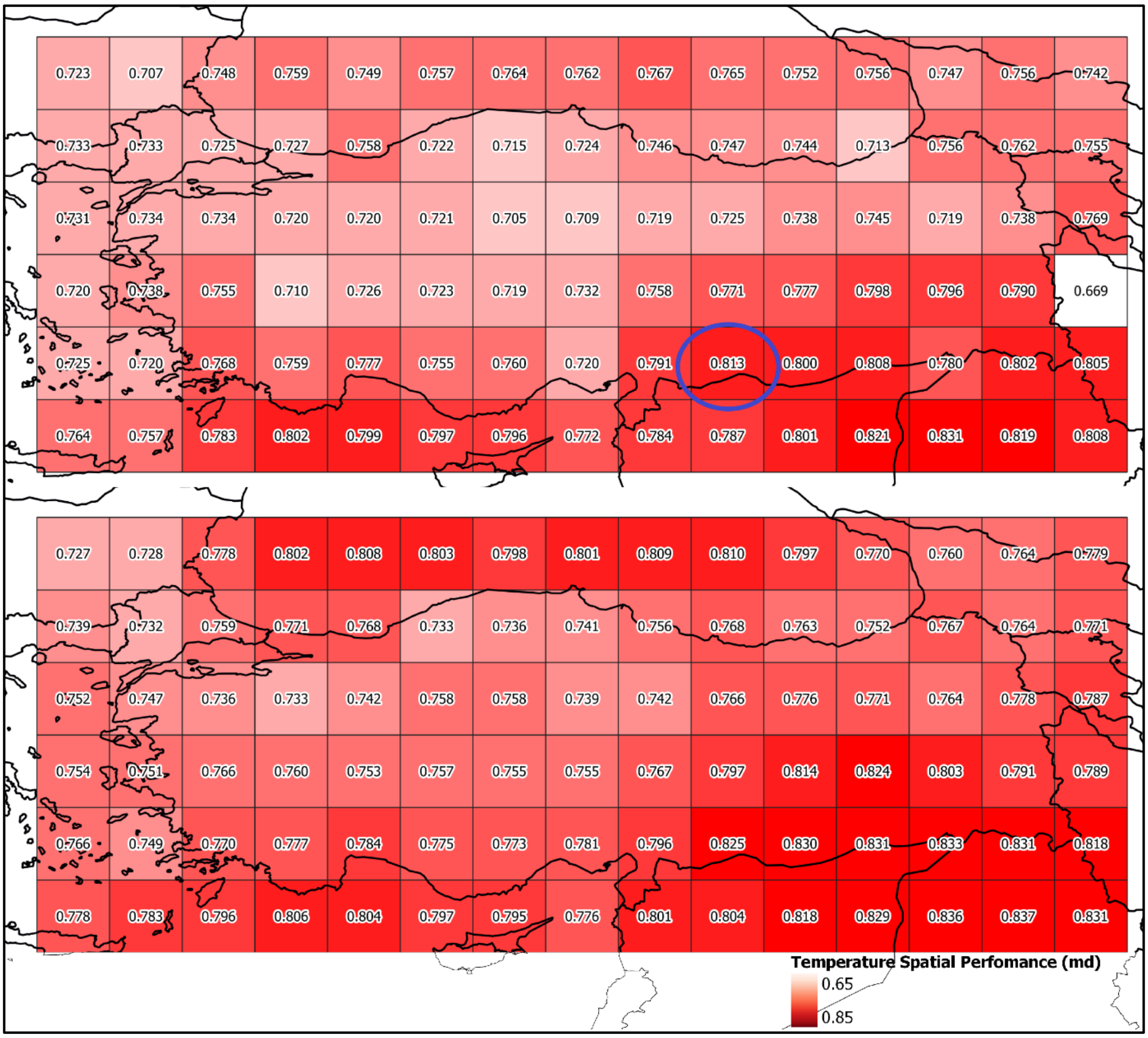

Figure 6. Raw (up) and bias corrected (down) modified index of agreement values for temperature (Blue circle represents best performed grid over Turkey)

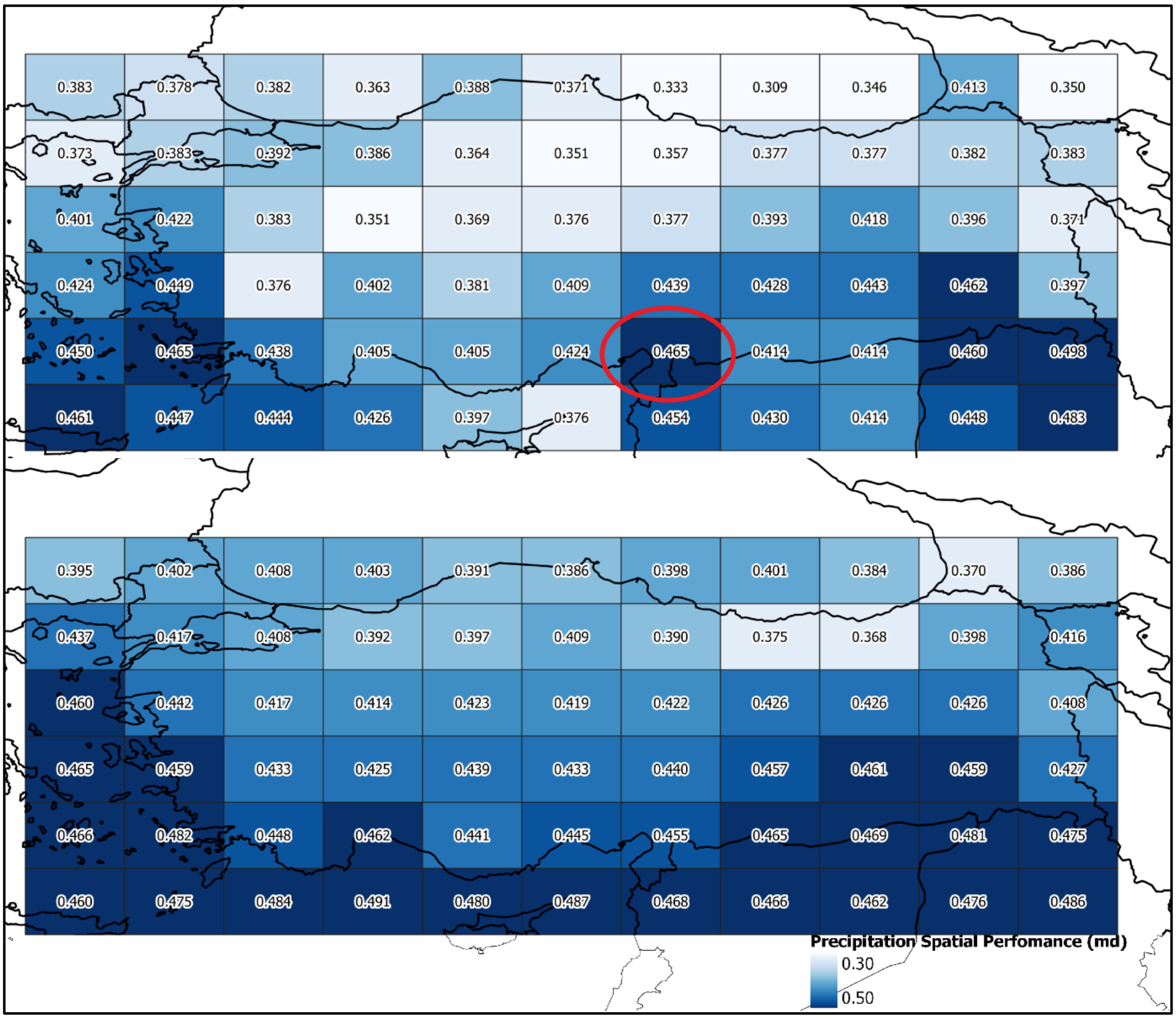

Figure 7. Raw (up) and bias corrected (down) modified index of agreement values for precipitation (Red circle represents best performed grid over Turkey).

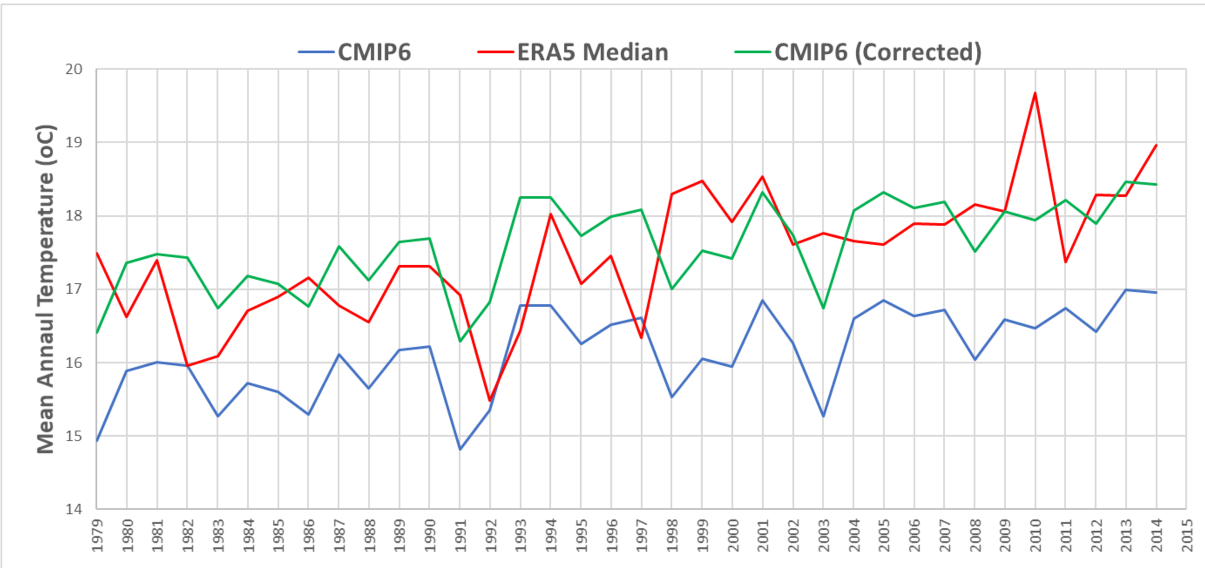

Figure 8. Mean annual temperature for historical period (1979-2004).

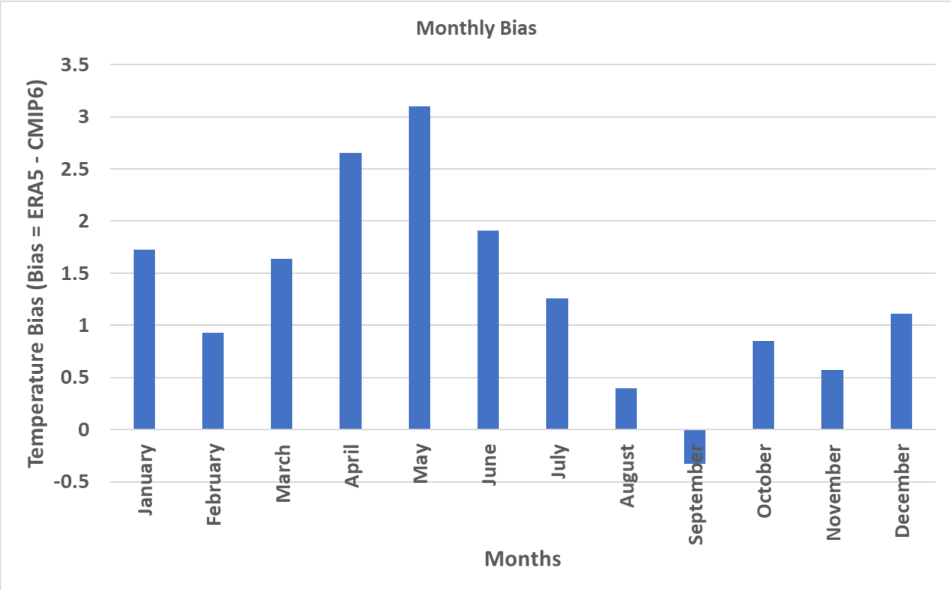

Figure 9. Temperature Biases of each month.

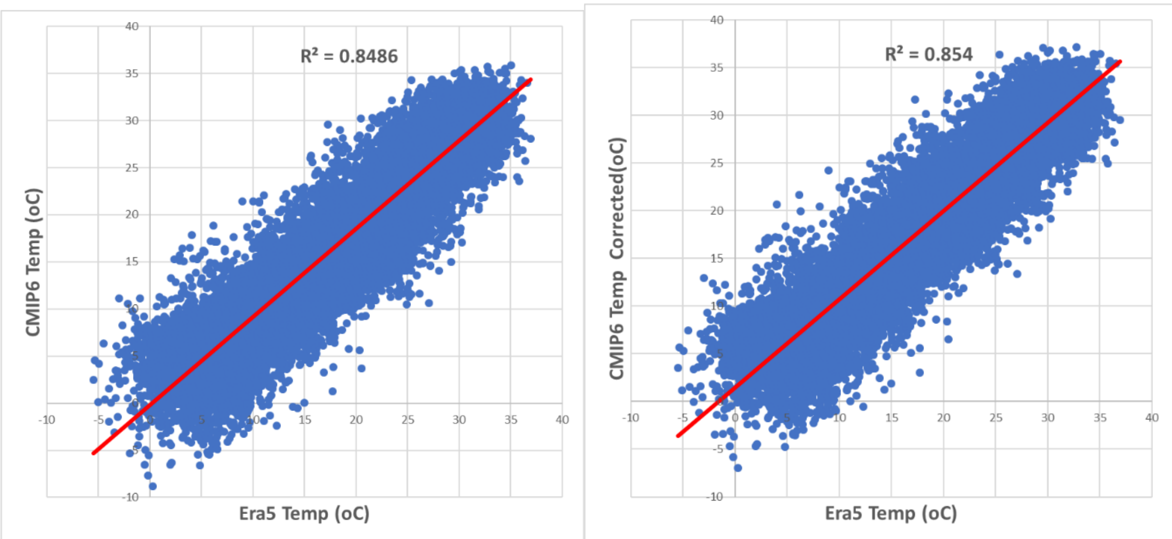

Figure 10. Scatter plot before and after bias correction for historical period (Daily).

CMIP6 original, ERA5 and CMIP6 bias corrected annual total precipitation values can be seen in Figure 11. After the bias is corrected on daily precipitation values, the comparison with the ERA5 data can be performed on monthly basis (Figure 12). It can be seen that CMIP6 temperature values underestimate the precipitation for all months except August. On daily basis, the bias correction improves the results compared to original CMIP6 daily precipitation values (Figure 13).

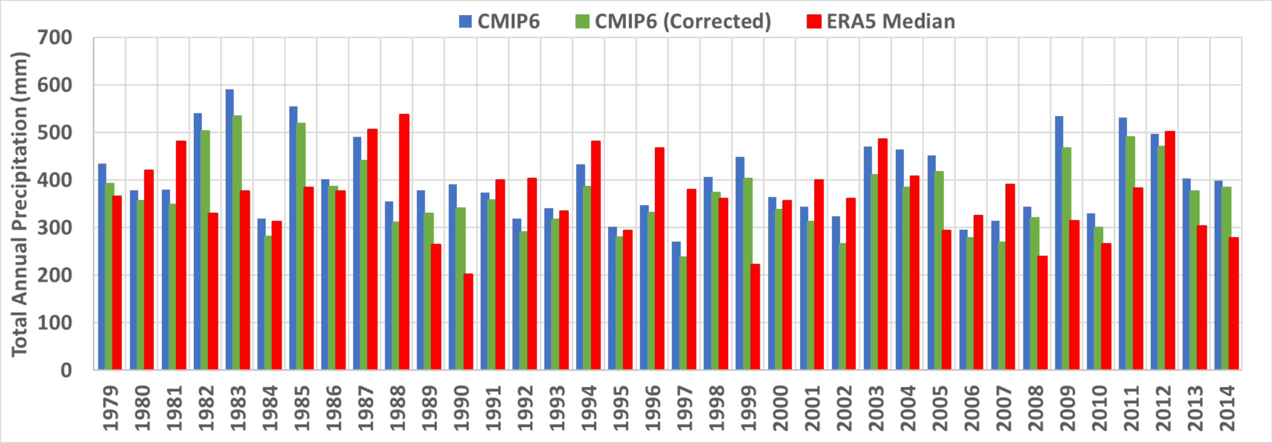

Figure 11. Annual total precipitation for historical period.

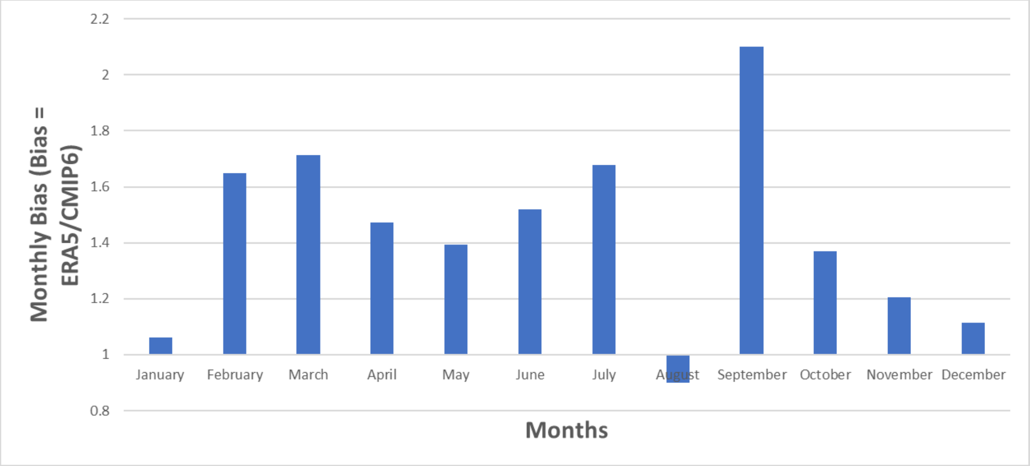

Figure 12. Monthly biases of each month for precipitation.

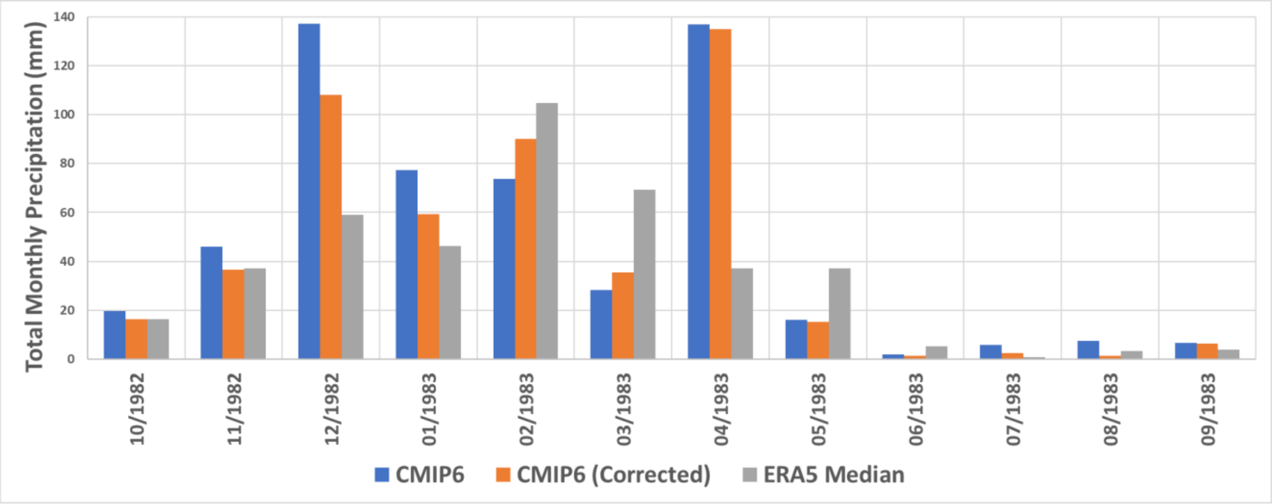

Figure 13. Daily monthly precipitation of historical period. (1982-1983)

3.6. Statistical downscaling

As statistical downscaling, the co-kriging method is applied. Co-kriging calculates estimates or predictions for a poorly sampled variable (the predictand) with help of a well-sampled variable (the covariate). Most importantly, the variables should be highly correlated. They can have positive or negative correlation. Elevation is used as covariate to downscale the temperature data of CMIP6 outputs. On the other hand, distance to the shoreline is used as an additional covariate for the precipitation downscaling.

i- Co-kriging Method

A model must be fitted to the data to approximately describe the spatial continuity of the data (Cameron and Hunter, 2002), since the kriging algorithm requires a positive definite model of spatial variability which can be called as variogram fitted model. A variogram is used to display the variability between data points as a function of distance.

Briefly, one tries to fit the spatially distributed data so that a model can understand the relation between the distance and the data as depicted in Figure 14.

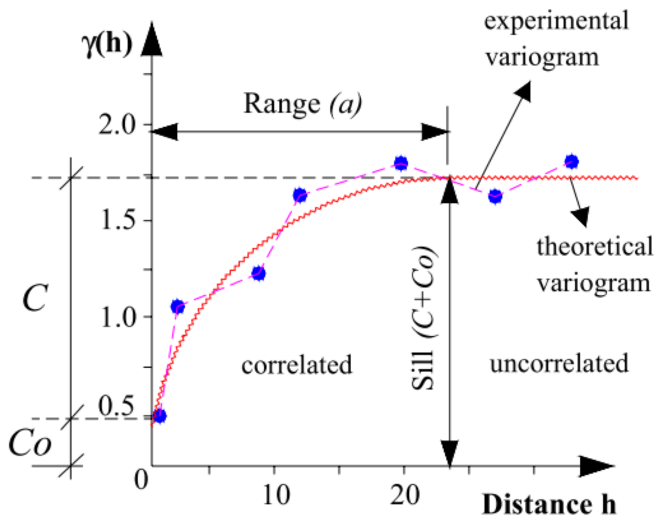

Figure 14. Theoretical and experimental fitted variogram. (Mendes & Lorandi, 2006)

There are three main parameters needed to fit the variogram model, which are mentioned as follows.

- Range (a): It is the distance between locations where variance no longer increases.
- Sill ($C + C_0$): It is the value of the variation chart. From that point, it can be assumed that there is no more spatial dependence (which should be carefully observed).
- Nugget (C_0): Describes the unexplained variance of the variable especially for short distances.

Second important point to mention is the selection of the mathematical model of variogram such as ‘exponential’, ‘spherical’ or ‘gaussian’ etc. Their differences can be seen in Figure 15.

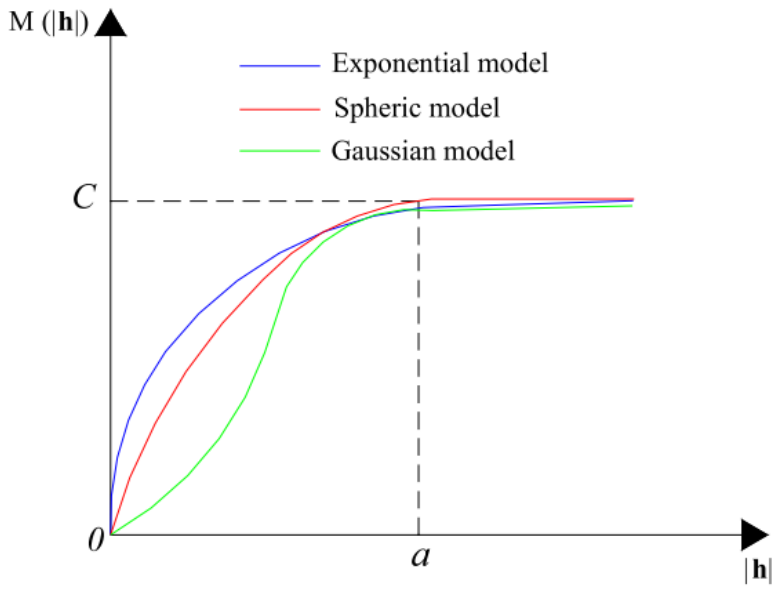

Figure 15. Different mathematical model fitting (Mendes & Lorandi, 2006).

In order to achieve the most convenient mathematical type and relevant coefficient of fitting model, R programming packages can be extremely useful. There are some packages to fit the model experimentally with researchers' trials and some automatic fitting packages to do it by own which will be mentioned.

ii- Preparing Daily Temperature Data

Bias corrected CMIP6 model (CNRM-ESM2) temperature data are used. The center points of grids are assumed as the representative values of that pixel for spatial calculations (Figure 16). The temperature values for January 1, 1979 are selected as an example. These points have temperature values of the CMIP6 output of the specific grids. For the temperature model (CNRM-ESM2) original spatial resolution is 1.40625°.

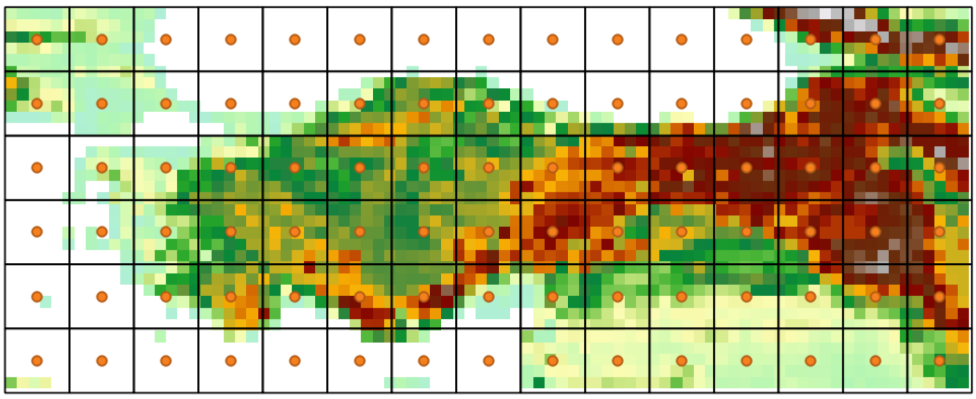

Figure 16. Grids and center points of bias corrected CMIP6 temperature values on DEM

The co-kriging is performed for the spatial resolution of ERA5 grids since the performance of the model is tested with the available ERA5 data. All of the elevation values come from Shuttle Radar Topography Mission (SRTM) data. These elevation values (median values were chosen to implement for grids) are used as covariate to make better prediction of downscaled CMIP6 output temperatures since the first assumption is temperature, which is directly correlated with elevation values, will be proved by statistical test in the following sections. The ERA5 grid points having 0.25° spatial resolution are presented in Figure 17 with the elevation values retrieved from SRTM are used as a covariant.

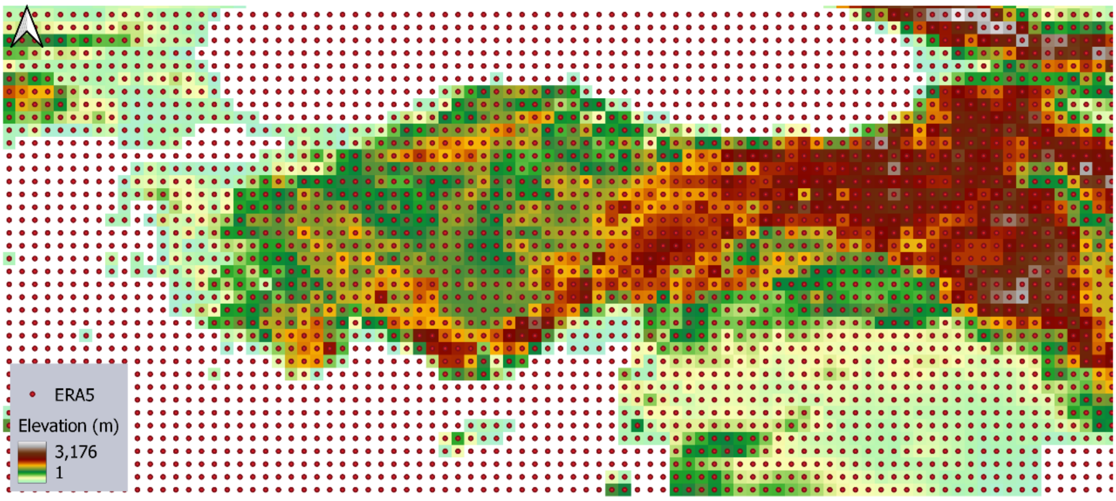

Figure 17. Grids and center points of ERA5 product on DEM (SRTM)

iii- Preparing Daily Precipitation Data

Bias corrected CMIP6 model (ACCESS-CM2) precipitation data are used. The precipitation values of February 1, 1979 are selected as an example. In addition to elevation, distance to shoreline is used as covariate for the downscaling of CMIP6 precipitation values. Distance to shoreline is calculated by using the v.distance processing tool of GRASS-GIS. Briefly, this tool uses two vector input data to calculate the closest distance from a vector to another one. In this case, the land boundaries and center points of grids were selected as inputs. Thereby, the tool finds the closest path from center points of grids to the land boundaries.

iv- Variogram Model Fitting

In order to implement co-kriging with auto-variogram approach, R programming codes are used [4].

The correlation coefficient between daily temperature and elevation for the selected date is calculated as -0.88 with a p value < 0.005. The daily temperature (Kelvin) and elevation (m) relation can be seen in Figure 18. The variogram with the relevant model and its coefficients are obtained (Figure 19).

[4] https://github.com/BerkayAkpinarr/Co-Kriging/blob/main/Co-KrigingR.R

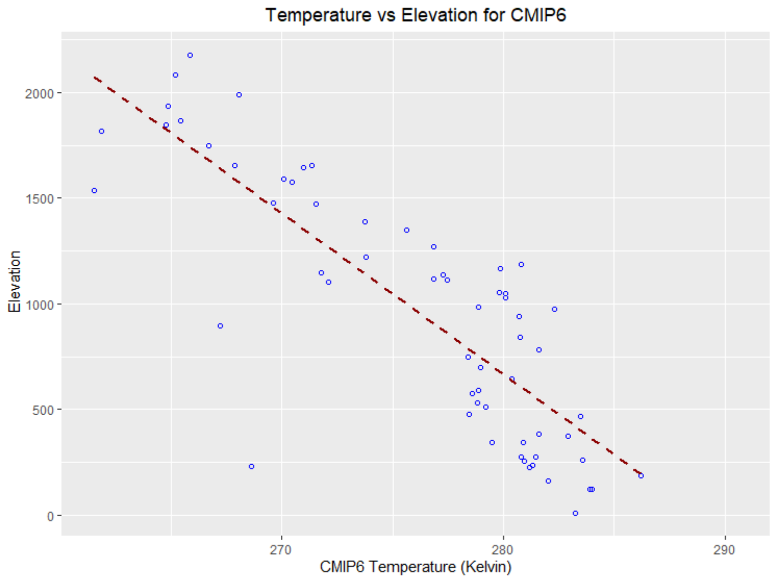

Figure 18. Daily Temperature (K) vs elevation (m) relation for bias corrected CMIP6 values for January 1, 1979

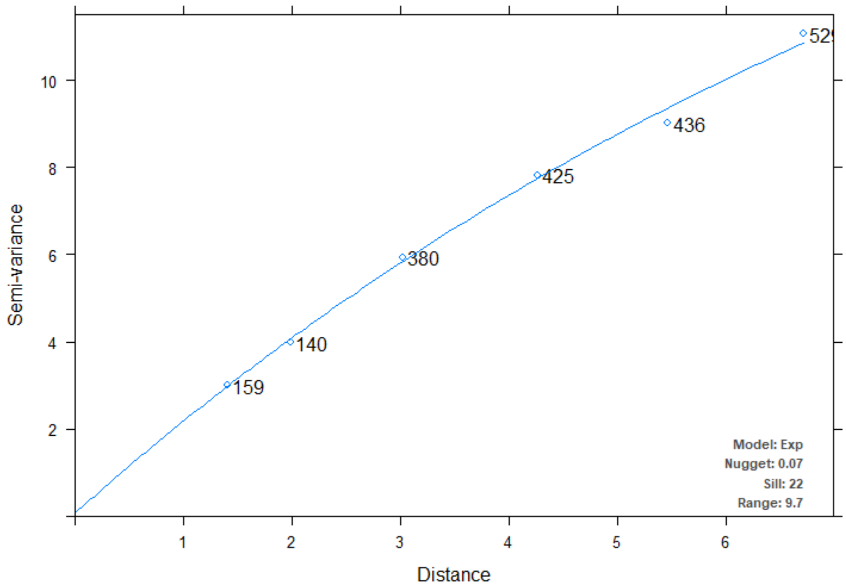

Figure 19. Fitted experimental and fitted variogram model.

After the variogram model is obtained, the bias corrected CMIP6 temperature values are interpolated to ERA5 grid size for the date of January 1, 1979 (Figure 20).

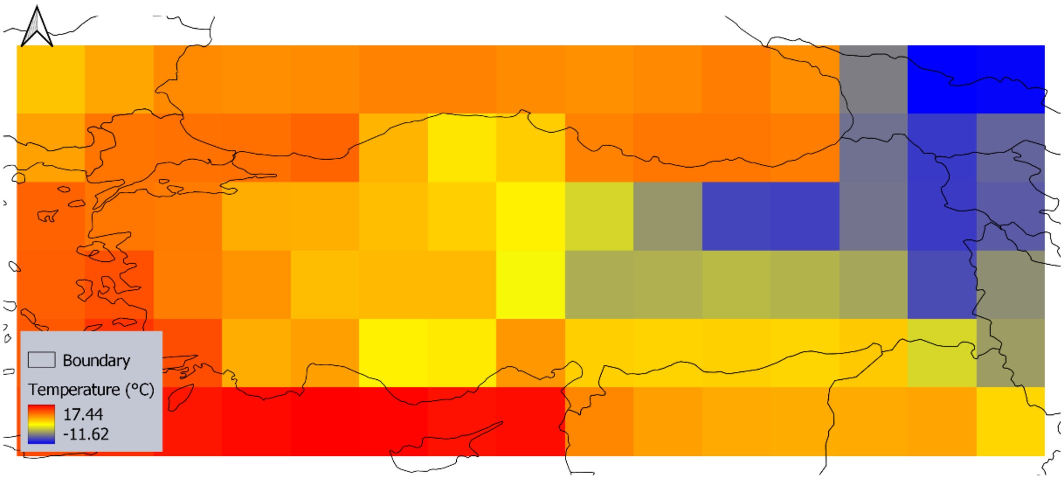

(a)

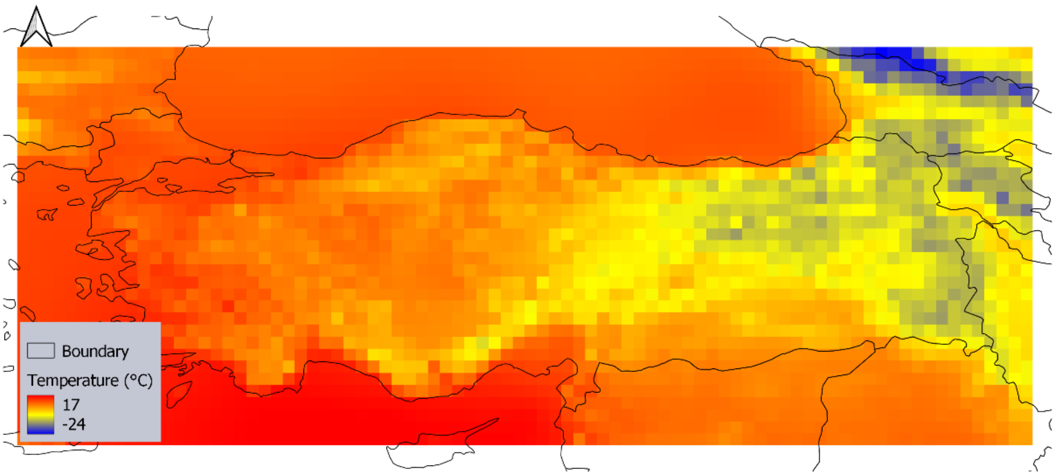

(b)

Figure 20. Bias corrected CMIP6 (a) and downscaled temperature values of CMIP6 outputs (b) for January 1, 1979.

As a comparison, absolute differences of the values of ERA5 – CMIP6 are depicted in Figure 21. A temperature output of bias corrected CMIP6 for January 1, 2025 is obtained and presented in Figure 22.

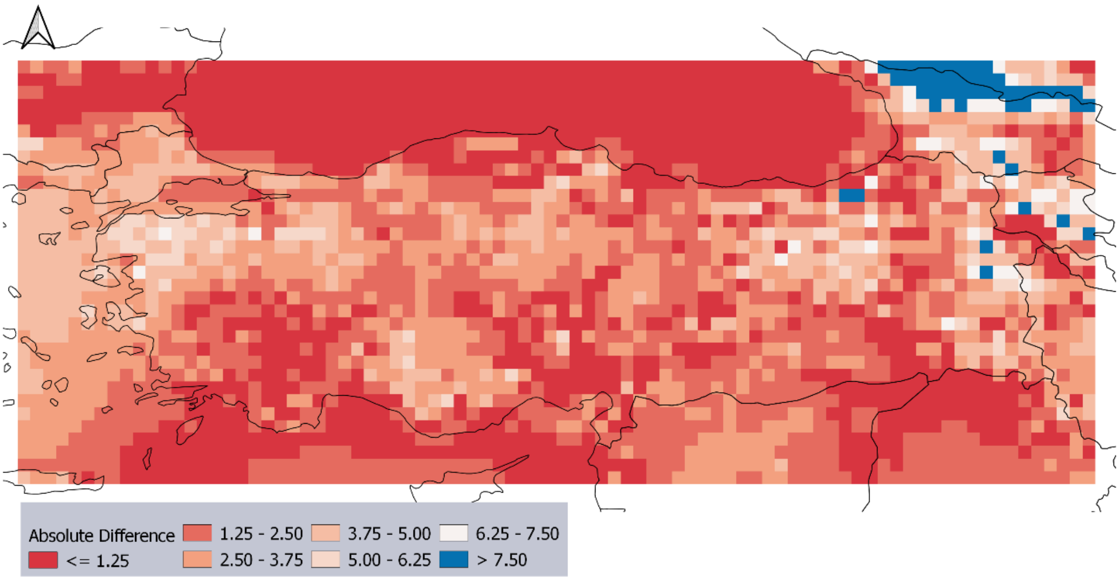

Figure 21. Absolute differences between temperature values of ERA5 and bias corrected CMIP6 data.

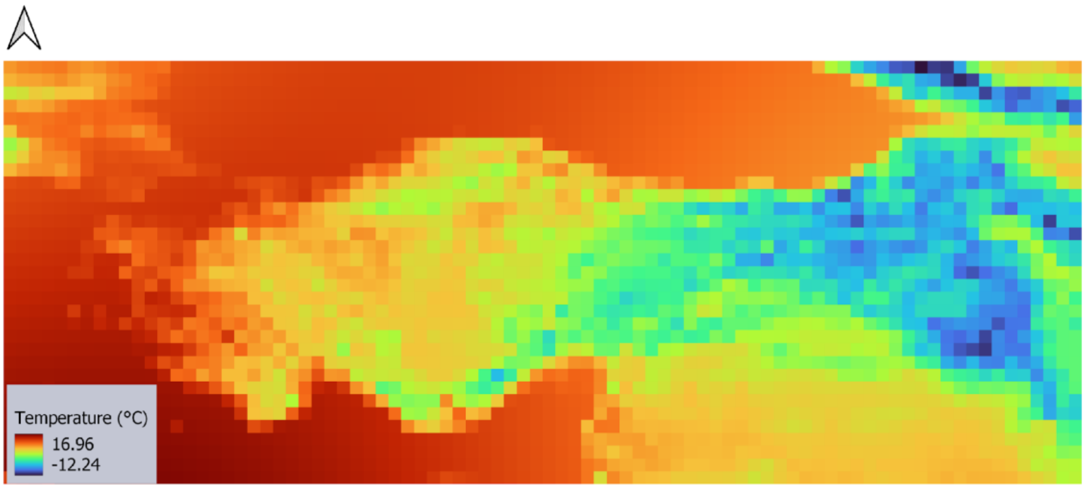

Figure 22. Co-kriged temperature output of CMIP6 for Jan 1, 2025.

Bias corrected CMIP6 precipitation data are also downscaled by using the same methodology. However, distance to shoreline is also added as a covariate for precipitation downscaling. It is important to determine whether the covariates (both elevation and distance to shoreline) are correlated with the precipitation or not. If this is not the case, variogram fitting may not give the correct results. Applying the correlation tests, for the CMIP6 precipitation case, it has been observed that both temperature and distance to shoreline are statistically correlated covariates as their p values are smaller than 0.1 as shown in Figure 23. The variogram with the relevant model and coefficients are given in Figure 24. After the variogram model is obtained, the bias corrected CMIP6 precipitation values are interpolated to ERA5 grid size for date February 1, 1979 (Figure 25).

	cmip6_values
cmip6_values	
elevation	0.0970
Distance	0.0031

Figure 23. P values of correlations of elevation and distance for precipitation downscaling.

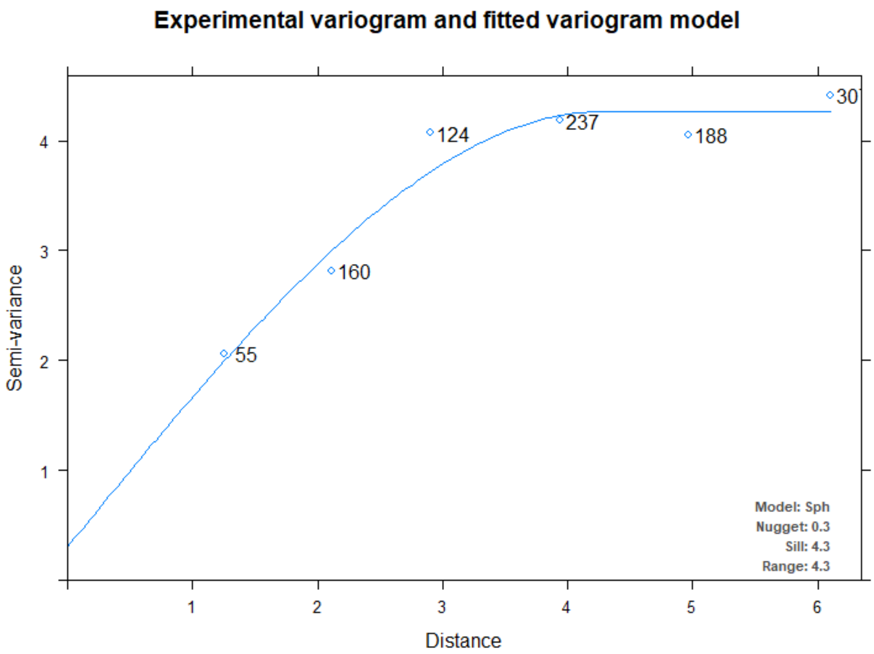

Figure 24. Experimental and fitted variogram for precipitation downscaling with covariates elevation and distance to shoreline.

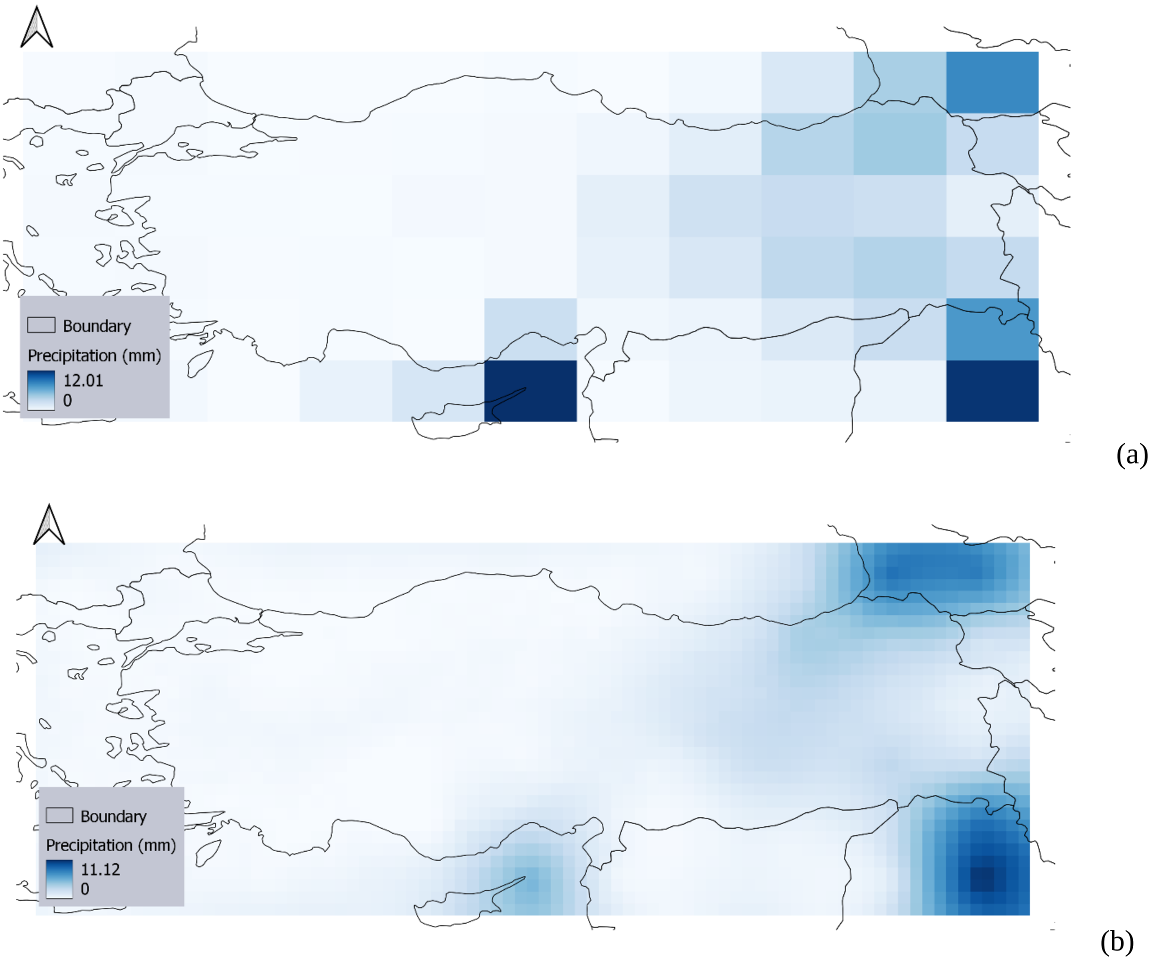

Figure 25. Bias corrected CMIP6 (a) and downscaled precipitation values of CMIP6 outputs for February 1,1979.

The absolute differences on February 1, 1979 for CMIP6 and ERA5 outputs are labeled in Figure 26.

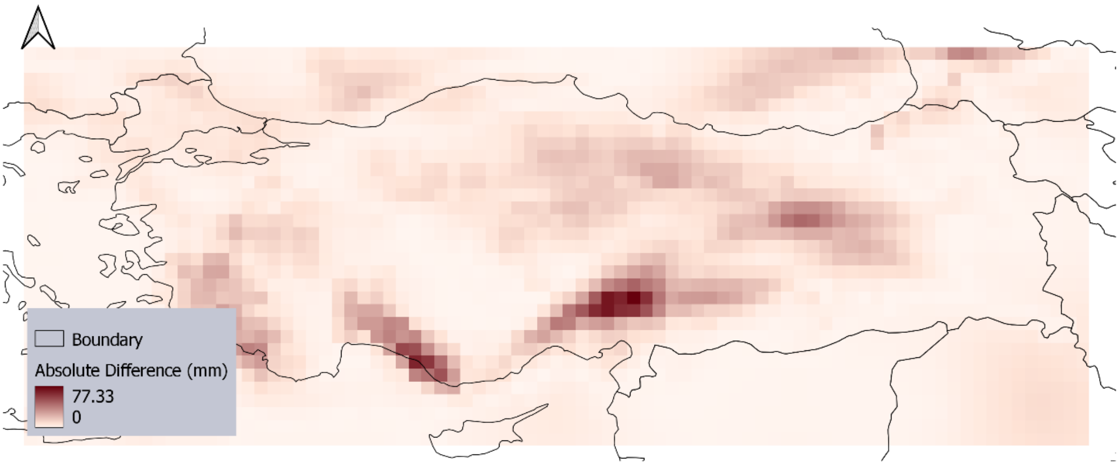

Figure 26. Absolute differences of precipitation of CMIP6 - ERA5 on February 1, 1979.

4. Conclusions

The statistical downscaling methodology to downscale the Global Climate Models' results to be used at pondscape scale is explained. Co-Kriging method is used, since additional observed variables (known as co-variates which are often correlated with the variable of interest) are used to improve the precision of the interpolation of the variable of interest. The co-variates presented in this report are examples and they may be region specific. The explanatory information can often improve the spatial interpolation of environmental variables; thus it is recommended to use explanatory variables. If some categorical variables (e.g. ecoregion, land use, etc.) are found important as explanatory variables, they must be converted to dummy variables which represent presence–absence of each category at any location within the study area with a 0 or 1.

In this report ERA5 reanalysis data are used as ground-based meteorological observations, since continuous data from the ground stations do not exist. The proposed methodology can be used for both ground observations or reanalysis products.

All the codes are provided in a GitHub repository.

5. References

Bağçaci, S. Ç., Yucel, I., Duzenli, E., & Yilmaz, M. T. (2021). Intercomparison of the expected change in the temperature and the precipitation retrieved from CMIP6 and CMIP5 climate projections: A Mediterranean hot spot case, Turkey. *Atmospheric Research*, *256*(March). https://doi. org/10.1016/j.atmosres.2021.105576

Bostan, P. A., Heuvelink, G.G.M. & Akyurek, Z. (2012). Comparison of regression and kriging techniques for mapping the average annual precipitation of Turkey. International Journal of Applied Earth Observation and Geoinformation. 19(115-126) http://dx.doi.org/10.1016/j.jag.2012.04.010

Cameron, K., & Hunter, P. (2002). Using spatial models and kriging techniques to optimize long-term ground-water monitoring networks: A case study. *Environmetrics*, *13*(5–6), 629–656. https://doi.org/10.1002/env.582

Daniels, A. E., Morrison, J. F., Joyce, L. A., Crookston, N. L., Chen, S. C., & McNulty, S. G. (2012). Climate projections FAQ. In *USDA Forest Service - General Technical Report RMRS-GTR* (Issue 277). https://doi.org/10.2737/RMRS-GTR-277

Dong, T., & Dong, W. (2021). Evaluation of extreme precipitation over Asia in CMIP6 models. *Climate Dynamics*, *57*(7–8), 1751–1769. https://doi.org/10.1007/s00382-021-05773-1

Eyring, V., Bony, S., Meehl, G. A., Senior, C. A., Stevens, B., Stouffer, R. J., & Taylor, K. E. (2016). Overview of the Coupled Model Intercomparison Project Phase 6 (CMIP6) experimental design and organization. *Geoscientific Model Development*, *9*(5), 1937–1958. https://doi.org/10.5194/gmd-9-1937-2016

Fan, X., Duan, Q., Shen, C., Wu, Y., & Xing, C. (2020). Global surface air temperatures in CMIP6: Historical performance and future changes. *Environmental Research Letters*, *15*(10). https://doi.org/10.1088/1748-9326/abb051

Fowler, H. J., Blenkinsop, S., & Tebaldi, C. (2007). Linking climate change modelling to impacts studies: Recent advances in downscaling techniques for hydrological modelling. *International Journal of Climatology*, *27*(12), 1547–1578. https://doi.org/10.1002/joc.1556

Gupta, H. V., Kling, H., Yilmaz, K. K., & Martinez, G. F. (2009). Decomposition of the mean squared error and NSE performance criteria: Implications for improving hydrological modelling. *Journal of Hydrology*, *377*(1–2), 80–91. https://doi.org/10.1016/j.jhydrol.2009.08.003

Ines, A. V. M., & Hansen, J. W. (2006). Bias correction of daily GCM rainfall for crop simulation studies. *Agricultural and Forest Meteorology*, *138*(1–4), 44–53. https://doi.org/10.1016/j.agrformet.2006.03.009

Kara F., Yucel, I. & Akyurek, Z. Climate change impacts on extreme precipitaiton of water supply area in Istanbul:use of ensemble climate modelling and geo-statistical downscaling. Hydrological Sciences Journal, 14(2481-2495). http://dx.doi.org/10.1080/02626667.2015.1133911

Karbalaye Ghorbanpour, A., Hessels, T., Moghim, S., & Afshar, A. (2021). Comparison and assessment of spatial downscaling methods for enhancing the accuracy of satellite-based precipitation over Lake Urmia Basin. *Journal of Hydrology*, *596*(February). https://doi.org/10.1016/j.jhydrol.2021.126055

Koch, J., Demirel, M. C., & Stisen, S. (2018). The SPAtial EFficiency metric (SPAEF): Multiple-component evaluation of spatial patterns for optimization of hydrological models. *Geoscientific Model Development*, *11*(5), 1873–1886. https://doi.org/10.5194/gmd-11-1873-2018

Kriegler, E., Bauer, N., Popp, A., Humpenöder, F., Leimbach, M., Strefler, J., Baumstark, L., Bodirsky, B. L., Hilaire, J., Klein, D., Mouratiadou, I., Weindl, I., Bertram, C., Dietrich, J. P., Luderer, G., Pehl, M., Pietzcker, R., Piontek, F., Lotze-Campen, H., … Edenhofer, O. (2017). Fossil-fueled development (SSP5): An energy and resource intensive scenario for the 21st century. *Global Environmental Change*, *42*, 297–315. https://doi.org/10.1016/j.gloenvcha.2016.05.015

Le Treut, H., Cubasch, U., & Allen, M. (2005). Historical Overview of Climate Change Science. *Notes*, *16*.

Legates, D. R., & McCabe, G. J. (1999). Evaluating the use of "goodness-of-fit" measures in hydrologic and hydroclimatic model validation. *Water Resources Research*, *35*(1), 233–241. https://doi.org/10.1029/1998WR900018

Liu, Y., Jing, W., Wang, Q., & Xia, X. (2020). Generating high-resolution daily soil moisture by using spatial downscaling techniques: a comparison of six machine learning algorithms. *Advances in Water Resources*, *141*, 103601. https://doi.org/10.1016/j.advwatres.2020.103601

Mendes, R. M., & Lorandi, R. (2006). Indicator kriging geostatistical methodology applied to geotechnics project planning. *IAEG 2006 Paper*, *527*, 1–12. http://iaeg2006.geolsoc.org.uk/cd/PAPERS/IAEG_527.PDF

Pang, B., Yue, J., Zhao, G., & Xu, Z. (2017). Statistical Downscaling of Temperature with the Random Forest Model. *Advances in Meteorology*, *2017*. https://doi.org/10.1155/2017/7265178

Patz, J. A., Campbell-Lendrum, D., Holloway, T., & Foley, J. A. (2005). Impact of regional climate change on human health. *Nature*, *438*(7066), 310–317. https://doi.org/10.1038/nature04188

Peng, J., Loew, A., Merlin, O., & Verhoest, N. E. C. (2017). A review of spatial downscaling of satellite remotely sensed soil moisture. *Reviews of Geophysics*, *55*(2), 341–366. https://doi.org/10.1002/2016RG000543

Riahi, K., van Vuuren, D. P., Kriegler, E., Edmonds, J., O'Neill, B. C., Fujimori, S., Bauer, N., Calvin, K., Dellink, R., Fricko, O., Lutz, W., Popp, A., Cuaresma, J. C., KC, S., Leimbach, M., Jiang, L., Kram, T., Rao, S., Emmerling, J., … Tavoni, M. (2017). The Shared Socioeconomic Pathways and their energy, land use, and greenhouse gas emissions implications: An overview. *Global Environmental Change*, *42*, 153–168. https://doi.org/10.1016/j.gloenvcha.2016.05.009

Sharma, M. A., & Singh, J. B. (2010). Use of Probability Distribution in Rainfall Analysis. *New York Science Journal*, *3*(9), 40–49.

Soriano, E., Mediero, L., & Garijo, C. (2019). Selection of bias correction methods to assess the impact of climate change on flood frequency curves. *Water (Switzerland)*, *11*(11). https://doi.org/10.3390/w11112266

Taylor, K. E., Stouffer, R. J., & Meehl, G. A. (2012). An overview of CMIP5 and the experiment design. *Bulletin of the American Meteorological Society*, *93*(4), 485–498. https://doi.org/10.1175/BAMS-D-11-00094.1

Trzaska, S., & Schnarr, E. (2014). A review of downscaling methods for climate change projections. *United States Agency for International Development by Tetra Tech ARD*, *September*, 1–42.

Tukimat, N. N. A., Ahmad Syukri, N. A., & Malek, M. A. (2019). Projection the long-term ungauged rainfall using integrated Statistical Downscaling Model and Geographic Information System (SDSM-GIS) model. *Heliyon*, *5*(9), e02456. https://doi.org/10.1016/j.heliyon.2019.e02456

Yang, B., Liu, H., Kang, E. L., Shu, S., Xu, M., Wu, B., Beck, R. A., Hinkel, K. M., & Yu, B. (2021). Spatio-temporal Cokriging method for assimilating and downscaling multi-scale remote sensing data. *Remote Sensing of Environment*, *255*(March), 112190. https://doi.org/10.1016/j.rse.2020.112190

You, Q., Cai, Z., Wu, F., Jiang, Z., Pepin, N., & Shen, S. S. P. (2021). Temperature dataset of CMIP6 models over China: evaluation, trend and uncertainty. *Climate Dynamics*, *57*(1–2), 17–35. https://doi.org/10.1007/s00382-021-05691-2